

Determining the Energy Gap between the Cis and Trans Isomers of HO₃⁻ Using Geometry Optimization within the Anti-Hermitian Contracted Schrödinger and Coupled Cluster Methods[†]

David A. Mazziotti*

Department of Chemistry and The James Franck Institute, The University of Chicago, Chicago, Illinois 60637

Received: July 31, 2007; In Final Form: October 14, 2007

The cis and trans isomers of the HO₃⁻ anion, which are important in proposed mechanisms for ozonization, are studied computationally. Relative energies, geometries, and normal-mode frequencies are calculated with anti-Hermitian contracted Schrödinger equation (ACSE) and coupled cluster methods. Both the ACSE method and the coupled cluster method with single and double excitations (CCSD) are applied in a correlation-consistent polarized double- ζ basis set (cc-pVDZ). Using coupled cluster with singles, doubles, and perturbative triples (CCSD(T)), we treat the problem with larger basis sets than those in previous work, including correlation-consistent polarized quadruple- ζ basis sets with (aug-cc-pVQZ) and without (cc-pVQZ) diffuse functions, which permit extrapolation of the cis and trans energies to the complete-basis-set limit. The cis isomer is found to be lower in energy than the trans isomer by -3.5 kcal/mol, which is 50% larger in magnitude than the best previous result of -2.2 kcal/mol. The bond lengths between the O₂ and OH fragments of the *cis*- and *trans*-HO₃ are calculated to be 1.713 and 1.857 Å, respectively, where both bond lengths are significantly longer than the 1.464 Å O–O bond in hydrogen peroxide. In this paper, we extend the ACSE method [Mazziotti, D. A. *J. Chem. Phys.* 2007, 126, 184101], which computes the two-electron reduced density matrix directly, to include geometry optimization by a Newton's method with numerical derivatives. Calculation of the *cis*- and *trans*-HO₃⁻ isomers by the ACSE yields energies, geometries, and frequencies that are closer to those from CCSD(T) than those from CCSD.

I. Introduction

The reaction of ozone with a substance is known as ozonization. Ozonization reactions have important roles in the following areas: (i) the study of air pollution, where ozone can react with pollutants,¹ (ii) the purification and treatment of water by ozone,² (iii) the beneficial and toxic effects of ozone in medicine,³ and (iv) chemical synthesis.⁴ Of particular importance are reactions of ozone with saturated organic molecules. Proposed mechanisms for these reactions^{1–4} involve the HO₃ radical, the HO₃⁻ anion, or derivatives of these molecules RO₃ and RO₃⁻, where R represents an organic functional group. While the HO₃ radical has been significantly studied both theoretically^{5,6} and experimentally,^{5,7} much less attention has been given to the HO₃⁻ anion.^{8–10}

An experiment using Fourier rotational spectroscopy in combination with theoretical calculations has recently shown that the trans isomer of the HO₃ radical is lower in energy than its cis isomer,⁵ where the cis and trans refer to the position of the hydrogen atom relative to the O₃ fragment of the molecule. From experimental rotational constants, the bond length between the O₂ and OH fragments of HO₃ is determined to be 1.688 Å,⁵ which is significantly longer than the 1.464 Å O–O bond in hydrogen peroxide.¹¹ In this paper, we study computationally the relative energies, optimized geometries, and normal-mode frequencies of the cis and trans isomers of the HO₃⁻ anion. Calculations are performed with methods based on the anti-Hermitian contracted Schrödinger equation (ACSE)^{12–14} and the

coupled cluster equations.¹⁵ Both the ACSE method and the coupled cluster method with single and double excitations (CCSD) are applied in a correlation-consistent polarized double- ζ basis set (cc-pVDZ).¹⁶ Using coupled cluster with singles, doubles, and perturbative triples (CCSD(T)), we treat the problem with larger basis sets than those in previous work, including correlation-consistent polarized quadruple- ζ basis sets with (aug-cc-pVQZ) and without (cc-pVQZ) diffuse functions,¹⁶ which permit extrapolation of the cis and trans energies to the complete-basis-set limit.¹⁷

The anti-Hermitian contracted Schrödinger equation (ACSE)^{12,13} has recently been solved for the two-electron reduced density matrix (2-RDM), its energies, and properties, without the many-electron wave function. In the ACSE, the 3-RDM is reconstructed as a functional of the 2-RDM by its cumulant expansion.^{18,19} In this paper, we extend previous work to optimize the ground-state energy from the ACSE with respect to molecular geometry. Molecular geometry optimization is implemented for the ACSE via a Newton's method with numerical gradients and Hessians. Calculations with the cis and trans isomers of HO₃⁻ by the ACSE yield energies and geometries that are closer to those from CCSD(T) than those from CCSD.

II. Theory

The formalism for solving the anti-Hermitian part of the contracted Schrödinger equation is presented in section II A, and a method for performing geometry optimization with the ACSE as well as the coupled cluster methods is developed in section II B.

[†] Part of the "Giacinto Scoles Festschrift".

* E-mail: damazz@uchicago.edu.

A. Anti-Hermitian Contracted Schrödinger Equation. The anti-Hermitian part of the contracted Schrödinger equation (ACSE)^{12–14} can be written as

$$\langle \Psi | [\hat{\Gamma}_{k,l}^{ij}, \hat{H}] | \Psi \rangle = 0 \quad (1)$$

where each index i represents a spin orbital that is the product of a spatial orbital and one of the two spin functions, α and β , and $[\]$ denotes the quantum mechanical commutator. Both the Hamiltonian operator \hat{H} and the elements of the two-electron reduced density operator (2-RDO) ${}^2\hat{\Gamma}$ are expressible in terms of the fundamental fermionic creation and annihilation operators

$$\hat{H} = \sum_{p,s} {}^1K_s^p a_p^\dagger a_s + \sum_{p,q,s,t} {}^2V_{s,t}^{p,q} a_p^\dagger a_q^\dagger a_t a_s \quad (2)$$

in which 1K and 2V denote a partitioning of the Hamiltonian into one- and two-electron operators, and

$${}^2\hat{\Gamma}_{k,l}^{ij} = a_i^\dagger a_j^\dagger a_t a_k \quad (3)$$

By rearranging the creation and annihilation operators, we can express the ACSE, as shown explicitly in ref 13, in terms of only the two- and three-electron reduced density matrices (2- and 3-RDMs)

$${}^2D_{k,l}^{ij} = \frac{1}{2} \langle \Psi | {}^2\hat{\Gamma}_{k,l}^{ij} | \Psi \rangle \quad (4)$$

and

$${}^3D_{p,q,s}^{i,j,k} = \frac{1}{6} \langle \Psi | {}^3\hat{\Gamma}_{p,q,s}^{i,j,k} | \Psi \rangle \quad (5)$$

where the elements of the 3-RDO are products of three creation and three annihilation operators

$${}^3\hat{\Gamma}_{p,q,s}^{i,j,k} = a_i^\dagger a_j^\dagger a_k^\dagger a_s a_q a_p \quad (6)$$

The 2- and 3-RDMs are normalized to $N(N-1)/2$ and $N(N-1)(N-2)/6$, respectively.

Solution of the ACSE for the ground-state energy and 2-RDM can be performed by solving a system of differential equations in a time-like variable λ .^{12,13} The system of equations can be interpreted as minimizing the energy through a sequence of unitary transformations, ordered by λ , that are applied to a reference wave function $\Psi(0)$, which can be either a single determinant, as in this paper, or a combination of determinants. Although these transformations can be understood in terms of their action on $\Psi(0)$, the differential equations depend only upon the 2- and 3-RDMs that are representable by a $\Psi(\lambda)$. The evolution equations for the energy and the 2-RDM are given by

$$\frac{dE}{d\lambda} = \langle \Psi(\lambda) | [\hat{H}, \hat{S}(\lambda)] | \Psi(\lambda) \rangle \quad (7)$$

and

$$\frac{d^2 D_{k,l}^{ij}}{d\lambda^2} = \langle \Psi(\lambda) | [{}^2\hat{\Gamma}_{k,l}^{ij}, \hat{S}(\lambda)] | \Psi(\lambda) \rangle \quad (8)$$

where

$$\hat{S} = \sum_{i,j,k,l} {}^2S_{k,l}^{ij} a_i^\dagger a_j^\dagger a_l a_k \quad (9)$$

and

$$\begin{aligned} {}^2S_{k,l}^{ij}(\lambda) &= -\frac{1}{\epsilon} \frac{\partial E(\lambda + \epsilon)}{\partial ({}^2S_{k,l}^{ij}(\lambda))} \Big|_{2S=0} \\ &= \langle \Psi(\lambda) | [{}^2\hat{\Gamma}_{k,l}^{ij}, \hat{H}] | \Psi(\lambda) \rangle \end{aligned} \quad (10)$$

At each λ , we select the elements defining the \hat{S} operator to minimize the energy along its gradient, where the ϵ in eq 10 is an arbitrarily small number. The right side of eq 10 is the residual of the ACSE in eq 1, and the right side of eq 8 is the residual of the ACSE with \hat{H} replaced by the anti-Hermitian $\hat{S}(\lambda)$. As shown in ref 12, eqs 7–10 can be expressed and evaluated in terms of their connected parts, the components which scale linearly with system size N .

To remove the indeterminacy of the differential equations from their dependence on the 3-RDM, we can reconstruct the 3-RDM from the 2-RDM by its cumulant expansion¹⁸

$${}^3D_{q,s,t}^{i,j,k} = {}^1D_q^i \wedge {}^1D_s^j \wedge {}^1D_t^k + 3{}^2\Delta_{q,s}^{ij} \wedge {}^1D_t^k + {}^3\Delta_{q,s,t}^{i,j,k} \quad (11)$$

where

$${}^2\Delta_{k,l}^{ij} = {}^2D_{k,l}^{ij} - {}^1D_k^i \wedge {}^1D_l^j \quad (12)$$

and the operator \wedge denotes the antisymmetric tensor product known as the Grassmann wedge product. The cumulant (or connected) part ${}^p\Delta$ of a p -RDM vanishes unless all p particles are statistically dependent, and hence, the amount of information in each cumulant p -RDM scales linearly with the number N of particles in the system. Second-order approximations of the cumulant 3-RDM in terms of the cumulant 2-RDM have been proposed by Nakatsuji and Yasuda,^{20,21} Mazziotti,^{21,22} and Valdemoro, Tel, and Perez-Romero.²³ All of these reconstructions are compared in nonminimal basis sets in a recent paper.¹⁹ Here, we use the Nakatsuji–Yasuda (NY) formula,^{20,21} which can be derived from the Mazziotti correction¹⁹

$${}^3\Delta_{q,s,t}^{i,j,k} \approx \frac{1}{6} \sum_l s_l \hat{A} ({}^2\Delta_{q,s}^{i,l} {}^2\Delta_{l,t}^{j,k}) \quad (13)$$

where s_l equals 1 if l is occupied in the Hartree–Fock reference and -1 if l is not occupied, and the operator \hat{A} performs all distinct antisymmetric permutations of the indices, excluding the summation index l . With the 3-RDM reconstruction, the system of differential equations for the ground-state energy and the 2-RDM can be evolved in λ without the many-electron wave function until either (i) the energy, (ii) the least-squares error of the ACSE, or (iii) the least-squares error of the 1,3-contracted Schrödinger equation^{13,14} increases.

B. Geometry Optimization. Optimization of molecular geometries is implemented for the ACSE through numerical differentiation. A simple Newton’s method is employed to update the geometry vector y

$$\Delta y = -H^{-1}g \quad (14)$$

where Δy is the change in the molecular geometry and g and H are the gradient vector and Hessian matrix of the ground-state energy as a function of the nuclear coordinates. The components of the gradient are computed by centered finite differences²⁴

$$g_i = \frac{E(y + h_i e_i) - E(y - h_i e_i)}{2h_i} \quad (15)$$

TABLE 1: The Energy Gaps between the Cis and Trans Isomers of HO_3^- , $E_{\text{cis}} - E_{\text{trans}}$, Are Reported for the Anti-Hermitian Contracted Schrödinger Equation (ACSE) Method with Cumulant Reconstruction of the 3-RDM with the Nakatsuji–Yasuda Correction, the Coupled Cluster Method with Single and Double Excitations (CCSD), and the Coupled Cluster Method with Single, Double, and Perturbative Triples (CCSD(T)) in a cc-pVDZ Basis Set and CCSD(T) in an aug-cc-pVQZ Basis Set

method	basis set	E_{cis} (au)	E_{trans} (au)	$E_{\text{cis}} - E_{\text{trans}}$ (au)	$E_{\text{cis}} - E_{\text{trans}}$ (kcal/mol)
ACSE	cc-pVDZ	-225.54489	-225.53355	-0.0113	-7.12
CCSD	cc-pVDZ	-225.52887	-225.51543	-0.0134	-8.43
CCSD(T)	cc-pVDZ	-225.55008	-225.54096	-0.00912	-5.72
	aug-cc-pVQZ	-225.90396	-225.89817	-0.00578	-3.63

where e_i is the unit vector with unity in the i th position and zeros elsewhere, the step sizes h_i are

$$h_i = \epsilon^{1/3} x_i \quad (16)$$

and the function $E(y)$ yields the energy evaluated with molecular geometry vector y . The parameter ϵ is the precision of the energy calculations, which scales each h_i to produce a gradient whose accuracy is nearly optimal for the precision available. Similarly, the elements of the Hessian matrix are computed by the first-order finite-difference formula²⁴

$$H_j^i = \frac{E(y + h_i e_i + h_j e_j) - E(y + h_i e_i) - E(y + h_j e_j) + E(y)}{h_i h_j} \quad (17)$$

where the step sizes h_i are

$$h_i = \epsilon^{1/4} x_i \quad (18)$$

Evaluation of the gradient g and the Hessian matrix H requires $2n$ and $n(n+1)/2 + n + 1$ energy evaluations (or solutions of the ACSE or coupled cluster equations), where n is the number of independent nuclear coordinates. In general, the Newton's method converges the energy within 10^{-8} in three–five iterations.

III. Applications

The energies, geometries, and normal-mode frequencies of the cis and trans isomers of singlet HO_3^- are explored in this section through the anti-Hermitian contracted Schrödinger equation (ACSE) method¹² with the Nakatsuji–Yasuda (NY) 3-RDM reconstruction^{19–21}, the coupled cluster method with single and double excitations (CCSD),¹⁵ and the coupled cluster method with single, double, and perturbative triples (CCSD(T)).¹⁵ The ACSE and CCSD were applied in a correlation-consistent polarized double- ζ (cc-pVDZ) basis set.¹⁶ The CCSD(T) was applied in this basis set, its augmented counterpart, as well as correlation-consistent polarized triple- and quadruple- ζ basis sets (cc-pVTZ and cc-pVQZ) and their augmented counterparts (aug-cc-pVTZ and aug-cc-pVQZ).¹⁶ Optimizations of the molecular geometries to minimize the ground-state energies of the isomers were performed in all cases with the numerical derivatives by the Newton's method outlined in section II B. The single-point energy calculations required by the geometry optimization were implemented by (i) the author's code for solving the ACSE by the method outlined in section II A and (ii) the coupled cluster codes in the PSI 3.3 package for quantum chemistry.²⁵ Electron integrals for the ACSE method were computed with GAMESS (U.S.A.).²⁶

Table 1 reports the energy gaps between the cis and trans isomers of HO_3^- , $E_{\text{cis}} - E_{\text{trans}}$. Each of the ACSE, CCSD, and CCSD(T) energies in Table 1 results from a molecular geometry optimization that requires approximately 150 single-point energy

TABLE 2: Two Complete-Basis-Set Extrapolations of the Energy Gaps between the Cis and Trans HO_3^- Isomers, $E_{\text{cis}} - E_{\text{trans}}$, Are Presented from CCSD(T) Calculations with Double- (cc-pVDZ and aug-cc-pVDZ), Triple- (cc-pVTZ and aug-cc-pVTZ), and Quadruple- ζ (cc-pVQZ and aug-cc-pVQZ) Basis Sets with and without Augmented Functions; the Energy Gaps from the Basis Set Extrapolations (cc-pVXZ Ex. and aug-pVXZ Ex.) are -3.54 and -3.52 kcal/mol, Respectively

basis set	E_{cis} (au)	E_{trans} (au)	$E_{\text{cis}} - E_{\text{trans}}$ (kcal/mol)	$E_{\text{cis}} - E_{\text{trans}}$ (kcal/mol)
cc-pVDZ	-225.55008	-225.54096	-0.00912	-5.72
cc-pVTZ	-225.80252	-225.79403	-0.00850	-5.33
cc-pVQZ	-225.88461	-225.87747	-0.00714	-4.48
cc-pVVXZ Ex.	-225.92417	-225.91852	-0.00565	-3.54
aug-cc-pVDZ	-225.65765	-225.65253	-0.00512	-3.21
aug-cc-pVTZ	-225.84553	-225.83972	-0.00581	-3.65
aug-cc-pVQZ	-225.90396	-225.89817	-0.00578	-3.63
aug-cc-pVXZ Ex.	-225.93033	-225.92471	-0.00561	-3.52

calculations. In the cc-pVDZ basis set, the ACSE energies for both cis and trans isomers are closer to the energies from CCSD(T) than those from CCSD. Consequently, the ACSE energy gap of -7.12 kcal/mol lies between the energy gaps of -8.43 and -5.72 kcal/mol of CCSD and CCSD(T), respectively. These ACSE results using geometry optimization further corroborate earlier single-point calculations that the ACSE with a second-order reconstruction improves upon the energies from CCSD, with greater improvement in larger basis sets.¹³ While each of these methods gives the energy of the cis isomer below the energy of the trans isomer, we also computed the energy gap by CCSD(T) in larger basis sets to examine the effect of increasing basis set size.

As shown in Table 2, geometry optimization calculations with CCSD(T) were performed in cc-pVXZ and aug-cc-pVXZ basis sets, where X = D, T, and Q. As the basis set size increased for cc-pVXZ, the absolute energy gap decreased from 5.72 to 4.48 kcal/mol. Interestingly, as the basis set increased for aug-cc-pVXZ, the absolute energy gap increased slightly from 3.21 to 3.63 kcal/mol. The addition of augmented functions decreased the magnitude of the energy gap because the diffuse functions stabilized the trans isomer more than the cis isomer. This difference in sensitivity to the diffuse functions is probably due to the longer bond length found in the trans isomer, as shown in Figure 1. Complete-basis-set limits can be extrapolated from these results by fitting them to the following exponential form¹⁷

$$a + b \exp(cx) \quad (19)$$

where x equals 2, 3, and 4 for cc-pVDZ (aug-cc-pVDZ), cc-pVTZ (aug-cc-pVTZ), and cc-pVQZ (aug-cc-pVQZ), respectively. As $x \rightarrow \infty$, the fitted parameter a equals the extrapolated energy. The energy gaps in these two complete-basis-set limits (cc-pVXZ Ex. and aug-cc-pVXZ Ex.), reported in Table 2, are -3.54 and -3.52 kcal/mol, respectively.

The optimized geometries of the cis and trans isomers of HO_3^- , described by the distances $r_{\text{O}_1\text{O}_2}$, $r_{\text{O}_2\text{O}_3}$, and $r_{\text{O}_3\text{H}}$ and the angles θ_{O_2} , θ_{O_3} , and τ , are shown in Table 3 for the ACSE,

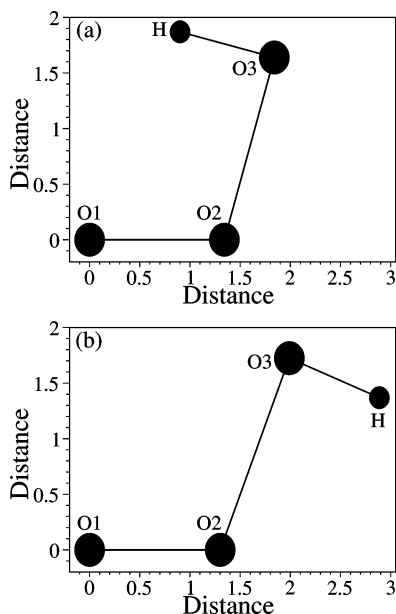


Figure 1. The geometries of the (a) cis and (b) trans isomers of HO_3^- are shown after geometry optimization by the CCSD(T) method in an aug-cc-pVQZ. Distances are reported in Å. Both the cis and trans structures exhibit long $r_{\text{O}_2\text{O}_3}$ bond lengths (1.713 and 1.857 Å) between the fragments O1–O2 and O3–H. In this basis set, the cis isomer is energetically more stable than the trans isomer by -3.63 kcal/mol. A previous study⁹ in a smaller basis set found an energy of -2.2 kcal/mol, which is 50% smaller in magnitude than the present gap, and a O2–O3 bond length of 1.803 Å in the cis isomer, which is significantly longer than the present bond length.

CCSD, and CCSD(T) methods in a cc-pVDZ basis set as well as for CCSD(T) in an aug-cc-pVQZ basis set. The angle θ_{O_2} indicates the angle formed by atom O2 with its two adjacent atoms; the dihedral angle τ , which is not shown in Table 3, is equal to 0 and 180° for the cis and trans isomers, respectively. In the cc-pVDZ basis set, the ACSE geometry parameters have values between those of CCSD and CCSD(T), which indicates that the ACSE improves upon the CCSD accuracy in both energy and geometry. An important aspect of both HO_3^- isomers is the long bond length $r_{\text{O}_2\text{O}_3}$, where a similarly long $r_{\text{O}_2\text{O}_3}$ bond length has been observed in the HO_3 radical.⁵ In the aug-cc-pVQZ basis set, the trans isomer has a slightly smaller distance $r_{\text{O}_1\text{O}_2}$ than that of the cis isomer, slightly wider angles θ_{O_2} and θ_{O_3} , and a significantly longer bond length $r_{\text{O}_2\text{O}_3}$. The shorter bond length $r_{\text{O}_2\text{O}_3} = 1.7125$ Å of the cis isomer supports its greater energetic stability. Figure 1 shows the geometries of the cis and trans isomers in the aug-cc-pVQZ basis set. In comparison to the results in the largest basis set, the ACSE and CCSD in the cc-pVDZ basis set underestimate $r_{\text{O}_2\text{O}_3}$, while CCSD(T) in the cc-pVDZ basis set overestimates $r_{\text{O}_2\text{O}_3}$. Calculations in slightly smaller basis sets, aug-cc-pVTZ and cc-pVQZ, indicate that the optimal geometries in aug-cc-pVQZ are fairly well converged with respect to basis set size.

The in-plane normal-mode frequencies of the cis and trans isomers of HO_3^- are shown in Table 4 for the ACSE, CCSD, and CCSD(T) methods in a cc-pVDZ basis set as well as for CCSD(T) in an aug-cc-pVQZ basis set. Because the Hessian matrices in the geometry optimization were computed in the internal coordinates given in Table 3, the normal-mode frequencies were computed by the general method described by Wilson, Decius, and Cross.²⁷ As with the energies and geometries, the normal-mode frequencies from the ACSE are between those from CCSD and CCSD(T) because the ACSE captures some “higher-excitation” effects that are not contained in CCSD. In

the aug-cc-pVQZ basis set, modes 2–4 have slightly higher frequencies for the cis than those for the trans, while modes 1 and 5 have slightly lower frequencies for the cis than those for the trans. The high frequency of mode 1 corresponds to the strong O–H bond stretch in both the cis and the trans isomers, while normal modes 4 and 5 with the lowest frequencies have large contributions from the stretch of the long O2–O3 bond. The frequency analysis confirms and quantifies the weakness of the long O2–O3 bonds.

IV. Discussion and Conclusions

Optimization of ground-state electronic energies with respect to molecular geometries with calculation of the normal modes has been implemented within the ACSE for computing optimal geometries and normal-mode frequencies of the cis and trans isomers of HO_3^- . Previous work had developed and implemented the ACSE for energy calculations at a single geometry or a series of geometries along the Born–Oppenheimer potential energy surface.^{12,13} Here, we extended these single-point calculations to geometry optimization and normal-mode frequency calculation through a Newton’s method with numerical derivatives. Components of the gradient were computed by centered finite differences, while components of the Hessian were computed by forward finite differences. At the optimal geometry, the normal modes and their frequencies were computed from the Hessian in internal coordinates by Wilson’s FG method.²⁷ The resulting geometry optimization method can be applied to a variety of electronic structure techniques including, as in the present work, coupled cluster methods. The energies at the optimal geometries of both the cis and trans isomers of HO_3^- support previous data that the ACSE improves significantly upon CCSD, especially as the basis set size increases.¹³

The energy gap between the cis and trans isomers of HO_3^- was studied by a variety of methods, ACSE, CCSD, and CCSD(T). For all methods and basis sets, the cis structure was found to be lower in energy than the trans structure. Larger basis sets, cc-pVQZ and aug-cc-pVQZ, than those employed in previous work⁹ permitted extrapolation of the cis and trans energies as well as their energy gap to the complete-basis-set limit. Extrapolations of energies from CCSD(T) both with and without diffuse functions gave an absolute energy gap of 3.5 kcal/mol between the cis (lower) and trans isomers. We obtained a gap that was 50% larger in magnitude than the 2.2 kcal/mol gap obtained by CCSD(T) in a smaller basis set in previous work.⁹ Calculations in ref 9 show that the cis isomer is stable against dissociation into HO^- and singlet O_2 ($^1\Delta_g$) by about 15.4 kcal/mol. Interestingly, the ordering of the cis and trans energies for HO_3^- contrasted with the ordering for the HO_3 radical, where spectroscopy and quantum calculations⁵ indicate that the trans structure is energetically more favorable than the cis isomer. Hence, the addition of an electron to the HO_3 radical causes the relative ordering of the cis and trans energies to switch.

Geometry optimization reveals a long bond length between the O_2 and OH fragments of the HO_3^- molecule. In the aug-cc-pVQZ basis set, the cis and trans isomers have 1.7125 and 1.8568 Å O2–O3 bond lengths, respectively. The weakness of the O2–O3 bond is reflected in the low frequencies of the two lowest normal modes of HO_3^- , each of which has a strong contribution from the stretch of the O2–O3 bond. The present calculations indicate that the bond length tends to decrease with the size of the basis set. The bond length of the cis isomer is shorter than the 1.803 Å O2–O3 bond length obtained in a smaller triple- ζ basis set in previous work,⁹ where the bond

TABLE 3: The Optimized Geometries of the Cis and Trans Isomers of HO₃⁻, Described by the Distances r_{O1O2} , r_{O2O3} , and r_{O3H} and the Angles θ_{O2} , θ_{O3} , and τ Are Shown for the ACSE, CCSD, and CCSD(T) Methods in a cc-pVDZ Basis Set as Well as for CCSD(T) in an aug-cc-pVQZ Basis Set; the ACSE Geometry Parameters Have Values between Those of CCSD and CCSD(T) in the cc-pVDZ Basis Set, and an Important Aspect of Both HO₃⁻ Isomers is the Long Bond Length r_{O2O3}

molecule	method	basis set	geometry parameters ^a				
			r_{O1O2}	r_{O2O3}	θ_{O2}	r_{O3H}	θ_{O3}
cis	ACSE	cc-pVDZ	1.4006	1.6108	103.53	0.97842	85.551
	CCSD	cc-pVDZ	1.4082	1.5499	103.17	0.97762	87.435
	CCSD(T)	cc-pVDZ	1.3465	1.7925	106.46	0.97368	81.493
		aug-cc-pVQZ	1.3431	1.7125	106.89	0.96702	86.905
trans	ACSE	cc-pVDZ	1.3173	1.8225	113.67	0.97302	87.929
	CCSD	cc-pVDZ	1.3122	1.7744	112.67	0.97054	90.367
	CCSD(T)	cc-pVDZ	1.3174	1.8848	114.80	0.97318	81.493
		aug-cc-pVQZ	1.3014	1.8568	111.79	0.96503	90.171

^a The dihedral angle τ , which is not displayed in the table, is equal to 0 and 180° for the cis and trans isomers, respectively.

TABLE 4: The In-Plane Normal-Mode Frequencies of the Cis and Trans Isomers of HO₃⁻ Are Shown in the Table for the ACSE, CCSD, and CCSD(T) Methods in a cc-pVDZ Basis Set as Well as for CCSD(T) in an aug-cc-pVQZ Basis Set^a

molecule	method	basis set	frequencies of in-plane normal modes (cm ⁻¹)				
			1	2	3	4	5
cis	ACSE	cc-pVDZ	3564.8	1250.8	881.7	497.2	164.6
	CCSD	cc-pVDZ	3524.9	1352.1	857.3	596.7	321.8
	CCSD(T)	cc-pVDZ	3598.6	1127.6	938.4	438.8	253.5
		aug-cc-pVQZ	3619.2	1154.9	924.8	464.9	152.5
trans	ACSE	cc-pVDZ	3597.4	1115.2	873.9	523.9	287.1
	CCSD	cc-pVDZ	3639.9	1100.2	906.8	500.9	268.7
	CCSD(T)	cc-pVDZ	3595.7	1100.9	807.8	486.4	253.3
		aug-cc-pVQZ	3661.5	1101.5	802.2	449.2	257.9

^a As with the energies and geometries, the normal-mode frequencies from the ACSE are between those from CCSD and CCSD(T) because the ACSE captures some "higher-excitation" effects that are not contained in CCSD. In the aug-cc-pVQZ basis set, modes 2–4 have slightly higher frequencies for the cis than the trans, while modes 1 and 5 have slightly lower frequencies for the cis than those for the trans. The high frequency of mode 1 corresponds to the strong O–H bond stretch in both the cis and the trans isomers, while normal modes 4 and 5 with the lowest frequencies have large contributions from the stretch of the long O2–O3 bond.

length was noted to be the longest known for a peroxide.¹¹ The corresponding O2–O3 bond length in the HO₃ radical, also long, has been shown from experimental rotational constants to be 1.688 Å.⁵ Despite the long bond length, multireference effects do not appear to be as important in HO₃⁻ as they are in the HO₃ radical. In the cc-pVDZ basis set, the occupation numbers of the 1-RDM from the ACSE deviate from 0 and 1 by, at most, ≈ 0.03 , and the absolute value of the largest two-particle transition amplitude in CCSD is ≈ 0.15 . Future work may be able to address the importance of these effects more completely through a recent extension of the ACSE method to treat multireference correlation.²⁸

In summary, the cis and trans isomers of the HO₃⁻ molecule have been studied in terms of their relative energies, geometries, and vibrational normal-mode frequencies with both the ACSE and coupled cluster methods. Importantly, the present work gives the first molecular geometry optimization by the ACSE method. The geometry optimization was performed with numerical derivatives of the ground-state energy with respect to internal coordinates. The ACSE calculations in this paper are based upon only the first revision¹³ of the ACSE code.¹² Future revisions of the code will include (i) further enhancement of efficiency and memory allocation, (ii) exploitation of molecular symmetry, and (iii) exploration of analytical derivatives within the geometry optimization. These advances will enable the treatment of larger basis sets, such as those treated by CCSD(T) in the present study, at a computational cost (r^6) closer to CCSD (r^6) than CCSD(T) (r^7), where r is the rank of the one-electron basis set.¹³ As shown in this work, the ACSE provides a new approach to the study of physical and chemical phenomena via the direct calculation of the 2-RDM and both its energy and its properties.

Acknowledgment. The author acknowledges Rajat Chaudhuri for helpful discussions on geometry optimization. The author also expresses his appreciation to Dudley Herschbach, Herschel Rabitz, John Coleman, and Alexander Mazziotti for their support and encouragement. The author thanks the NSF, ACS Petroleum Research Fund, the Henry–Camille Dreyfus Foundation, the Alfred P. Sloan Foundation, and the David–Lucile Packard Foundation for their support.

References and Notes

- (1) (a) Rowland, F. S. *Angew. Chem., Int. Ed. Engl.* **1996**, *35*, 1786. (b) Molina, M. *Angew. Chem., Int. Ed. Engl.* **1996**, *35*, 1779. (c) Crutzen, P. *Angew. Chem., Int. Ed. Engl.* **1996**, *35*, 1758. (d) Seinfeld, J. H. *Science* **1989**, *243*, 745. (e) McGregor, K. G.; Anastasio, C. *Atmos. Environ.* **2001**, *35*, 1091.
- (2) (a) Gottschalk, C.; Libra, J. A.; Saupe, A. *Ozonation of Drinking Water and of Wastewater*; Wiley-VCH: New York, 2000. (b) Munoz, F.; Mvula, E.; Braslavsky, S. E.; von Sonntag, C. *J. Chem. Soc., Perkin Trans 2* **2001**, 1109. (c) Pietsch, J.; Sacher, F.; Schmidt, W.; Brauch, H.-J. *Water Res.* **2001**, *35*, 3537.
- (3) Bocci, V. *Arch. Med. Res.* **2007**, *38*, 265.
- (4) Bailey, P. S. *Ozonation in Organic Chemistry*; Academic Press: New York, 1982; Vol. II.
- (5) Suma, K.; Sumiyoshi, Y.; Endo, Y. *Science* **2005**, *308*, 1885.
- (6) (a) Blint, R. J.; Newton, M. D. *J. Chem. Phys.* **1973**, *59*, 6220. (b) Mathisen, K. B.; Siegbahn, P. E. M. *J. Chem. Phys.* **1984**, *90*, 225. (c) Dupuis, M.; Fitzgerald, G.; Hammond, B.; Lester, W. A.; Schaefer, H. F., III. *J. Chem. Phys.* **1986**, *84*, 2691. (d) Vincent, M. A.; Hillier, I. H. *J. Phys. Chem.* **1995**, *99*, 3109. (e) Jungkamp, T. P. W.; Seinfeld, J. H. *Chem. Phys. Lett.* **1996**, *257*, 15. (f) Setokuchi, O.; Sato, M.; Matuzawa, S. *J. Phys. Chem. A* **2000**, *104*, 3204. (g) Silveira, D. M.; Caridade, P. J. S. B.; Varandas, A. J. C. *J. Phys. Chem. A* **2004**, *108*, 8721. (h) Chalmet, S.; Ruiz-Lopez, M. F. *ChemPhysChem* **2006**, *7*, 463.
- (7) (a) Cacace, F.; de Petris, G.; Pepi, F.; Troiani, A. *Science* **1999**, *285*, 81. (b) Nelander, B.; Engdahl, A.; Svensson, T. *Chem. Phys. Lett.* **2000**, *332*, 403. (c) Murray, C.; Derro, E. L.; Sechler, T. D.; Lester, M. I. *J. Phys. Chem. A* **2007**, *111*, 4727.

- (8) (a) Mathisen, K. B.; Gropen, O.; Skancke, P. N.; Wahlgren, U. *Acta Chem. Scand. A* **1983**, *37*, 817. (b) Koller, J.; Plesnicar, B. *J. Am. Chem. Soc.* **1996**, *118*, 2470.
- (9) Kraka, E.; Cremer, D.; Koller, J.; Plesnicar, B. *J. Am. Chem. Soc.* **2002**, *124*, 8462.
- (10) Cacace, F.; Cipollini, R.; de Petris, G.; Troiani, A. *Int. J. Mass Spectrom.* **2003**, *228*, 717.
- (11) Koput, J. *J. Mol. Spectrosc.* **1986**, *115*, 438.
- (12) (a) Mazziotti, D. A. *Phys. Rev. Lett.* **2006**, *97*, 143002. (b) Mazziotti, D. A. *Phys. Rev. A* **2007**, *75*, 022505. (c) Mazziotti, D. A. In *Reduced-Density-Matrix Mechanics: With Application to Many-Electron Atoms and Molecules, Advances in Chemical Physics*; Mazziotti, D. A., Ed.; Wiley: New York, 2007; Vol. 134, Chapter 12. (d) Valdemoro, C.; Tel, L. M.; Alcoba, D. R.; Pérez-Romero, E. In press.
- (13) Mazziotti, D. A. *J. Chem. Phys.* **2007**, *126*, 184101.
- (14) (a) Colmenero, F.; Valdemoro, C. *Phys. Rev. A* **1993**, *47*, 979. (b) Nakatsuji, H.; Yasuda, K. *Phys. Rev. Lett.* **1996**, *76*, 1039. (c) Mazziotti, D. A. *Phys. Rev. A* **1998**, *57*, 4219.
- (15) Crawford, T. D.; Schaefer, H. F. In *Reviews in Computational Chemistry*; Lipkowitz, K. B., Boyd, D. B., Eds.; Wiley-VCH: New York, 2000; Vol. 14.
- (16) (a) Dunning, T. H., Jr. *J. Chem. Phys.* **1989**, *90*, 1007. (b) Kendall, R. A.; Dunning, T. H., Jr.; Harrison, R. J. *J. Chem. Phys.* **1992**, *96*, 6796.
- (17) Klopper, W.; Helgaker, T. *Theor. Chem. Acc.* **1998**, *99*, 265.
- (18) (a) Mazziotti, D. A. *Chem. Phys. Lett.* **1998**, *298*, 419. (b) Mazziotti, D. A. *Int. J. Quantum Chem.* **1998**, *70*, 557. (c) Kutzelnigg, W.; Mukherjee, D. *J. Chem. Phys.* **1999**, *110*, 2800.
- (19) DePrince, A. E., III; Mazziotti, D. A. *J. Chem. Phys.* **2007**, *127*, 104104.
- (20) Yasuda, K.; Nakatsuji, H. *Phys. Rev. A* **1997**, *57*, 2648.
- (21) Mazziotti, D. A. *Phys. Rev. A* **1999**, *60*, 3618.
- (22) Mazziotti, D. A. *Chem. Phys. Lett.* **2000**, *326*, 212.
- (23) Valdemoro, C.; Tel, L. M.; Pérez-Romero, E. In *Many-Electron Densities and Density Matrices*; Cioslowski, J., Ed.; Kluwer: Boston, MA, 2000.
- (24) Dennis, J. E.; Schnabel, R. B. *Numerical Methods for Unconstrained Optimization and Nonlinear Equations*; SIAM: Philadelphia, PA, 1987.
- (25) Crawford, T. D.; Sherrill, C. D.; Valeev, E. F.; Fermann, J. T.; King, R. A.; Leininger, M. L.; Brown, S. T.; Janssen, C. L.; Seidl, E. T.; Kenney, J. P.; Allen, W. D. *J. Comput. Chem.* **2007**, *28*, 1610.
- (26) Schmidt, M. W.; Baldrige, K. K.; Boatz, J. A.; Elbert, S. T.; Gordon, M. A.; Jensen, J. H.; Koseki, S.; Matsunaga, N.; Nguyen, K. A.; Su, S.; Windus, T. L.; Dupuis, M.; Montgomery, J. A., Jr. *J. Comput. Chem.* **1993**, *14*, 1347.
- (27) Wilson, E. B.; Decius, J. C.; Cross, P. C. *Molecular Vibrations: The Theory of Infrared and Raman Vibrational Spectra*; McGraw-Hill: New York, 1955.
- (28) Mazziotti, D. A. *Phys. Rev. A* **2007**, *76*, 052502.